

5—1

Hybrid Defect Detection Method based on Shape Measurement and Feature Extraction for Complex Patterns

Hilário Haruomi KOBAYASHI^{†1}, Yasuhiko HARA^{†1}, Hideaki DOI^{†1}

Production Engineering Research Laboratory, Hitachi Ltd.

Kazuo TAKAI^{†2} and Akiyoshi SUMIYA^{†2}

Telecommunication Division, Hitachi Ltd.

Abstract

Visual inspection of printed circuit boards (PCBs) at the final production stage is necessary for quality assurance and the requirements for an automated inspection are very high. However, consistent inspection of patterns on these PCBs is very difficult due to pattern complexity. Most of the previously developed techniques are not sensitive enough to detect defects in complex patterns. To solve this problem, we propose a new optical system that discriminates pattern types existing on a PCB, such as copper, solder resist and silk-screen printing. We also developed the hybrid defect detection technique to inspect discriminated patterns. This technique is based on shape measurement and features extraction methods. We used the proposed techniques in an actual automated inspection system, realizing real time transactions with a combination of hardware equipped with image processing LSIs, and PC software. Evaluation with this inspection system ensures a 100% defect detection rate and a fairly low false alarm rate (0.06%). The present paper describes the inspection algorithm and briefly explains the automated inspection system.

1. Introduction

Visual inspection of printed circuit boards (PCBs) at the final production stage is necessary for quality assurance and the needs for automated inspections are very high in the electronics industry. Several vision-based inspection techniques¹⁾⁻³⁾ have been developed and systems using these techniques have integrated in the intermediate stages of PCB manufacturing. However, there has been little attempt to integrate them in the final stage of production. This is because inspection at this stage is very difficult, due to the PCBs different materials and the different characteristics of surface textures and colors, which leads to complex images. Figure 1 shows a typical PCB with a surface consisting primarily of three types of patterns on the substrate. These patterns consist of copper wiring, solder resists and marks produced by silk-screen printing. Each type of pattern must be examined with appropriate inspection criteria.

^{†1}Address: 292 Yoshida-cho Totsuka-ku, Yokohama 244-0817 Japan. E-mail: hilario@perl.hitachi.co.jp

^{†2}Address: 216 Totsuka-cho, Totsuka-ku, Yokohama 244-8567 Japan

Gray scale⁴⁾ and color-based⁵⁾ inspection techniques were developed to inspect PCBs at the final manufacturing stage. The gray scale inspection technique uses the index space method⁶⁾, originally used to inspect color printed matter such as pre-paid cards. The color-based inspection technique compares RGB color data with reference data. Fundamentally, both techniques are based on pixel comparison between detected and reference patterns. The above-mentioned reference patterns are usually obtained from more than one good previously selected circuit board. These systems do not have enough flexibility to apply different inspection criteria for each pattern type.

At present, no commercial system with a satisfactory performance is available for this task and such inspection and quality control is done off-line by human operators. In addition to being expensive and time-consuming, the results of such inspection are also somewhat subjective due to fatigue and the limitation of human vision.

In this paper, we describe a new optical system that discriminates pattern types existing on a PCB, and we describe the inspection algorithm. The newly developed system increases efficiency by making use of both shape measurement and feature extraction, thereby exploiting the strengths and overcoming weaknesses of each method. This system also provides advantages by covering a large variety of defects compared to those covered by using each method alone.

The proposed method is highly effective at finding defects in PCBs.

2. Defects on PCBs and technical issues

Table 1 shows typical defects that must be detected on PCBs. The major technical issue concerning an inspection algorithm is to achieve accurate and reliable inspection of

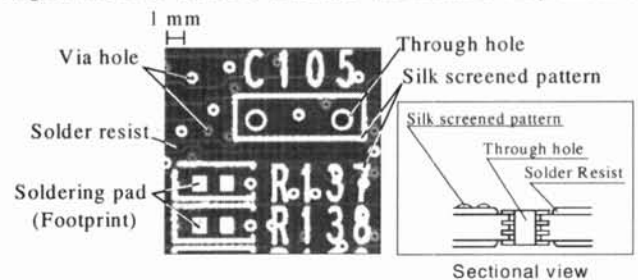


Fig. 1. Sample of the Printed Circuit Board

several types of patterns, as follows:

- (1) There are two different technologies currently being used in manufacturing for connecting components: surface-mounting (SMT) and through-hole (THT) technologies. In SMT, tolerances in placement and fixation of the components are especially tight because the probability of device movement after placement is high. Thus, soldering pads, used for SMT devices, must be submitted to a more severe inspection than those used for through-hole patterns. Therefore, pattern recognition is necessary to allow inspection based on criteria according to the type of the patterns.
- (2) Inspection criteria for silk-screen printed patterns are subjective and do not need to be so tight, when compared to those for copper patterns. In this paper, we define the quantitative inspection criteria as listed in Table 1.

In the next sections we will explain in detail the developed system, from pattern detection to effective defect detection.

3. Pattern detection

Figure 2 shows the special optical system developed. In order to obtain discriminated pattern images with high signal-to-noise ratios, fluorescence detection⁷⁾ and reflected light detection methods were utilized. The differences between the two methods are summarized in Table 2.

It is known that dielectric material like solder resists and silk-screened patterns emit fluorescent light when submitted to short wavelength radiation. Therefore, when using fluorescence detection with violet light illumination for excitation, solder resists and silk-screened patterns are bright and copper patterns are dark. Optical fibers, band pass filters (exciter filter) and lenses were used to illuminate the PCB with violet light (436 nm) generated from a short-arc mercury lamp. The outlet of the fiber is rectangular in shape so as to illuminate the inspection area effectively. Dichroic mirrors were designed to guide violet light on the PCBs and to transmit emitted fluorescent light (500~600 nm).

On the other hand, when using reflected light detection with red light (630~780 nm), solder resist areas have low reflectivity due to high absorption within this wavelength range. In contrast, white colored materials, such as silk-screened patterns and copper patterns, have high reflectivity throughout the red wavelength range.

Red light illumination is carried out using a pair of LED (Light Emission Diode) arrays arranged in parallel, with angles of 45° and 135° relative to the PCB surface. The characteristic wavelength of this LED array was 660 nm.

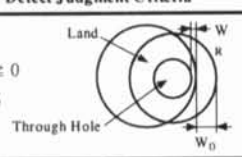
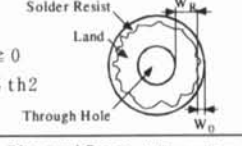
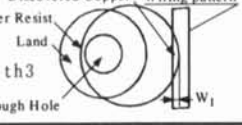
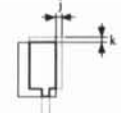
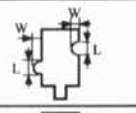


In this optical system, images from the two detection systems are taken simultaneously by two highly sensitive linear sensors (2048 pixels) arranged in parallel. The image pixel size is 26 μm.

4. Image processing algorithm

Figure 3 shows the basic inspection algorithm flow. Detected signals are processed in two channels in parallel and they have following steps.

- (1) First step: preprocessing of the detected images;
- (2) Second step: pattern separation. The images are

Tab. 1. Pattern defect judgment criteria

No.	Pattern Type	Defect Mode	Defect Judgment Criteria
1	Through Hole Land	Solder Resist Overlapped [On Half Moon Shape]	$WR \geq 0$ $W0 \leq th1$ 
2	"	Solder Resist Overlapped [On Ring Shape]	$WR \geq 0$ $W0 \leq th2$ 
3	"	Solder Resist Discovered [Mousebite]	Discovered Copper, Wiring pattern $W1 \leq th3$ 
4	Soldering Pad (footprint)	Solder Resist Overlapped or Pattern Displacement	Width $J \leq thw1$ Length $K \leq thL1$ 
5	"	Mousebite or/and Protuberance	$W \leq thW2$ $L \leq thL2$ 
6	"	Pinhole/Isolated Blob	$L \leq thL$ 
7	On Solder Resist	Dirty/Scattering	$L \leq thD$
8	Silk screened Pattern	Mousebite or Protuberance	$thM \leq 2L \times L$ $2L$ L: pattern width 

Tab. 2 Illumination effects on the patterns

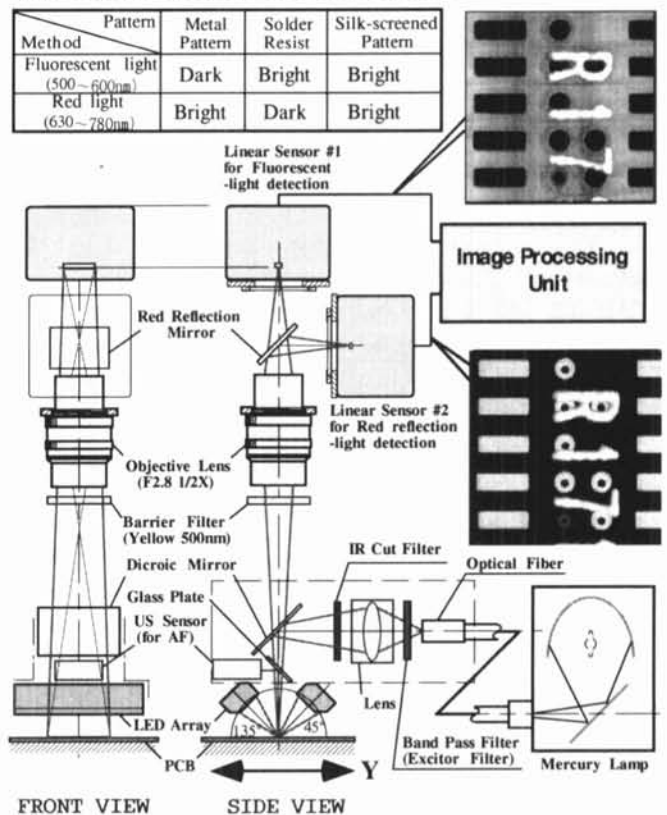


Fig. 2. Optical system for image detection

discriminated to metal and silk-screened pattern to inspected separately;

- (3) Third step: Defect detection. For metal patterns our proposed algorithm has basically two parts: feature extraction and shape measurement, while for silk-screened patterns we compare detected patterns with reference patterns generated from CAD data.

Still in the metal pattern inspection, the feature extraction method based on operators templates is highly sensitive to small defects, but covering a great variety of defect type and sizes makes the procedure computationally expensive. On the other hand, shape measurement method is suitable for normal and larger pattern shape defects, but can not detect smaller ones. This issue is overcome with conjoint use of both of the two methods.

Operational details of each step of the defect detection are described in the next subsections.

4.1 Preprocessing of the detected image

Shading compensation is carried out for the fluorescent light signal and red light signal, separately. Differences in the sensitivity of the sensors are compensated, including the non-uniformity in the illumination of the lighting system. This shading compensation stabilizes the detected signal over the entire detection area.

4.2 Pattern separation

After the thresholding process, copper and silk-screened patterns can be obtained separately by using pixel calculations for images acquired by the two detection methods. The details of the pattern separation are shown in Figure 4. Here, defects on the solder resist can be found as deficiencies in the copper pattern images. Therefore, discrimination for the two pattern types described above is enough for inspection purposes. The algorithm proposed below is used in defect detection.

4.3 Features extraction

This procedure is aimed at detecting small defects, such as scattered resist on a copper pattern, especially on SMT devices such as soldering pad.

The defect detectors of this method are performed by three types of operators as shown in Figure 5.

(a) Shape deformation defect detection

A set of operators is designed to detect smaller defects on pattern boundaries in four directions (0° , 90° , 180° , and 270°) as shown in Figure 5(a).

From operator's pixels for pattern edge extraction, we calculate,

$$\text{edge } C_i = \{ (\bar{c}_i) \cap (c'_i) \} \quad (1)$$

$$\text{edge } D_i = \{ (\bar{d}_i) \cap (d'_i) \} \quad (2)$$

here, the inner pattern is white (WHT=1) and the background is black (BLK=0). Consider n_c as the total of cases when $\text{edge } C_i=1$ and n_d as the total of cases when $\text{edge } D_i=1$. If

$$n_c \geq n_0 \cap n_d \geq n_0 \quad (3)$$

is satisfied to predefined criterion value n_0 , then we conclude that the operator is effectively on edge of the pattern. Under this condition, if

$$(f_1) \cap (f_2) \cap (f_3) = 1 \quad (4)$$

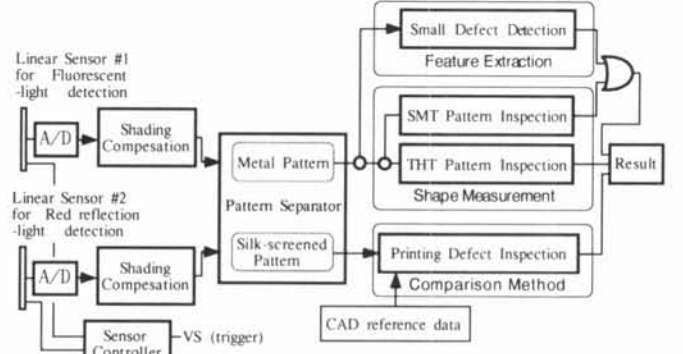


Fig. 3. Inspection algorithm flow

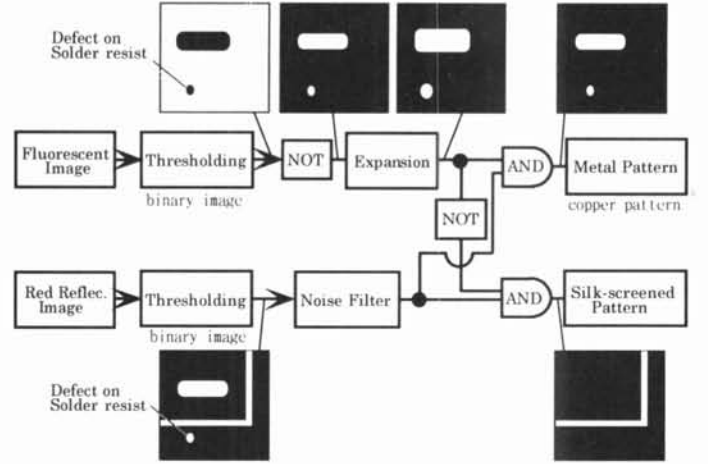


Fig. 4. Pattern separation flow

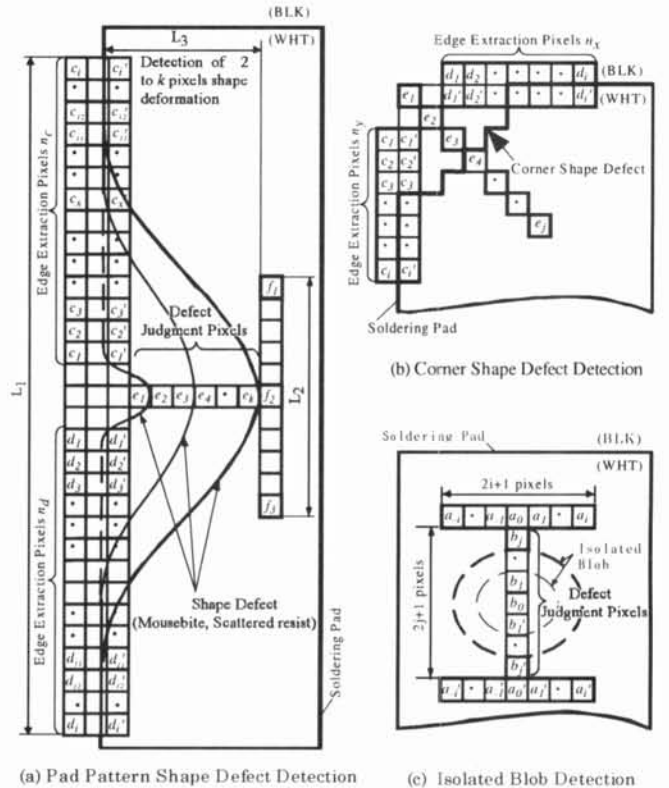


Fig. 5. Operators to detect pattern shape defects

is satisfied, then we must verify the defect judgment pixels e_k as follows:

$$\text{edge } E_1 = \{ (\bar{e}_1) \cap (e_2) \}$$

$$\dots$$

$$\text{edge } E_j = \{ (\bar{e}_j) \cap (e_{j+1}) \} \quad (5)$$

$$\text{edge } E_k = \{ (\bar{e}_k) \cap (f_2) \}$$

E_j is defined as the first j of edge $E_j=1$. If

$$E_j \geq E_{j_0} \quad (6)$$

is satisfied for predefined E_{j_0} , then we judge that there is shape deformation defect on the pattern.

The final result of extraction is a logical AND of the four direction features. This operator also detects isolated blobs or pin hole defects.

(b) Corner shape defect detection

The operator described above works effectively for the lateral side of the pattern but not for corner defects. The operator in Figure 5(b) is introduced to cover corner defects. They occur in the four directions (0° , 90° , 180° , and 270°).

From operator's pixels for corner edge extraction, we calculate,

$$\text{edge } Y_i = \{ (\bar{c}_i) \cap (c'_i) \} \quad (7)$$

$$\text{edge } X_i = \{ (\bar{d}_i) \cap (d'_i) \} \quad (8)$$

and consider n_y as the total of cases when edge $Y_i=1$, and n_x as the total of cases when edge $X_i=1$. If

$$n_y \geq k_0 \cap n_x \geq k_0 \quad (9)$$

is satisfied for the predefined value of k_0 , then we conclude that the operator is effectively on the corner of the pattern. Under this condition, we must verify the defect judgment pixels e_k as follows:

$$\text{edge } E_k = \{ (\bar{e}_k) \cap (e_{k+1}) \} \quad (10)$$

E_k is defined as the first k of edge $E_k=1$. If

$$E_k \geq E_{k_0} \quad (11)$$

is satisfied for the predefined E_{k_0} , then we judge that there is a corner defect on the pattern.

As in (a), the final result of defect extraction is a logical AND of the four direction features.

(c) Isolated blob detection

To detect small pinhole or isolated blob type defects, we introduce the operators shown in Figure 5(c). These operators are available in two directions (0 , 90°).

We calculate,

$$A_i = (a_{-i}) \cap \dots \cap (a_{-1}) \cap (a_0) \cap (a_1) \dots \cap (a_i) \quad (12)$$

$$A'_i = (a'_{-i}) \cap \dots \cap (a'_{-1}) \cap (a'_0) \cap (a'_1) \dots \cap (a'_i) \quad (13)$$

If, $(A_i) \cap (A'_i) = 1$ and, if

$$H_j = |(b_j) \cup \dots (b_1) \cup (b_0) \cup (b'_1) \dots \cup (b'_j)| = 1$$

are satisfied, there is a defect on the pattern.

The sizes of the operators described above are not fixed and can be regulated by setting limits for length, orientations and width of patterns.

All of these 10 operators are implemented on only one chip LCA (Logic Circuit Array). Each one of these operators is numbered. When defect is detected, this

number is tagged to data as a detector code. The results are given as defect position coordinates and detector code.

4.4 Shape measurement

This method labels the metal pattern and measures the shape features. Here, the shape of a pattern is represented by measurements of center of mass (CM), size of bounding rectangle, area, compactness, perimeter and 1st degree moments. In this paper we define compactness as the ratio of pattern area and area of bounding rectangle. For each measurement, an identification code is established.

As shown in Figure 6, for each labeled pattern, a table of measured features is constructed. Labeling and feature measurement are carried out by hardware in parallel with image processing LSIs, keeping transactions in real time.

Because linear image sensors were used in order to attain the image, the PCB is mounted on a stage that allows continuous movement in the Y direction as shown in Figure 7. This movement is synchronized with sensor line scan in the X direction, obtaining a continuous image.

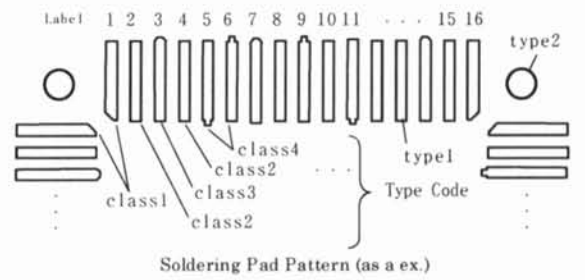
Due to the structural characteristics of the LSIs used, image processing was done sequentially, by reading each sub-image (frame) from the entire scanned page. Patterns detected partially must be codified together with its complementary part, which is located in the next frame. Once identified the patterns to be codified as individual ones, the combination of their measured features is made.

For example, to obtain combined CM of the pattern fragmented in two parts, we calculate the geometric average of the CMs as follows:

$$(X_m, Y_m) = \left(\frac{S' \cdot X'_m + S'' \cdot X''_m}{S' + S''}, \frac{S' \cdot Y'_m + S'' \cdot Y''_m}{S' + S''} \right) \quad (14)$$

where, (X_m, Y_m) is CM and S is pattern area. Single and double quotation represent values on the previous and next frame, respectively.

The results were transferred to a PC, which made a table of characteristics sets per labeled pattern. In the PC, the tables were compared with a corresponding reference



Soldering Pad Pattern (as an ex.)

Pattern Shape Data Table

Label	Characteristics Set			Classification	
	C.Mass	size	...	type*	class
1	(x_1, y_1)	Lx_1, Ly_1	...	1	1
2	(x_2, y_2)	Lx_2, Ly_2	...	1	2
3	(x_3, y_3)	Lx_3, Ly_3	...	1	3
4	(x_4, y_4)	Lx_4, Ly_4	...	1	2
5	(x_5, y_5)	1	4
...	0	...

(*Through Hole Pad=0, Foot Print Pad=1, Others=2)

Fig. 6. Pattern shape measurement and classification

table generated in advance from CAD data in order to evaluate the pattern defects. The correspondence between the reference and detected pattern is made by CM. The position tolerance was defined as the region determined by bounding rectangle.

The above comparison is made by evaluating distance metric of characteristics set for each detected pattern with respect to respective reference data. If exist at least one feature data that does not satisfy the criteria, pattern coordinates are reported as defect data with identification code of the measurement.

The above-mentioned CAD data describes the PCB pattern by aperture definition, exposure, and movement command of the photoplotter. The reference data has the following steps and characteristics:

- (1) Round-off processing⁸⁾ is applied to the bitmapped data of the metal pattern, generated from CAD data, making the shape of the reference data similar to the one of the detected pattern. Next, labeling and shape measurement are carried out to construct the reference table.
- (2) Data on pattern type and class codes are added to reference table to allow recognition of THT and SMT

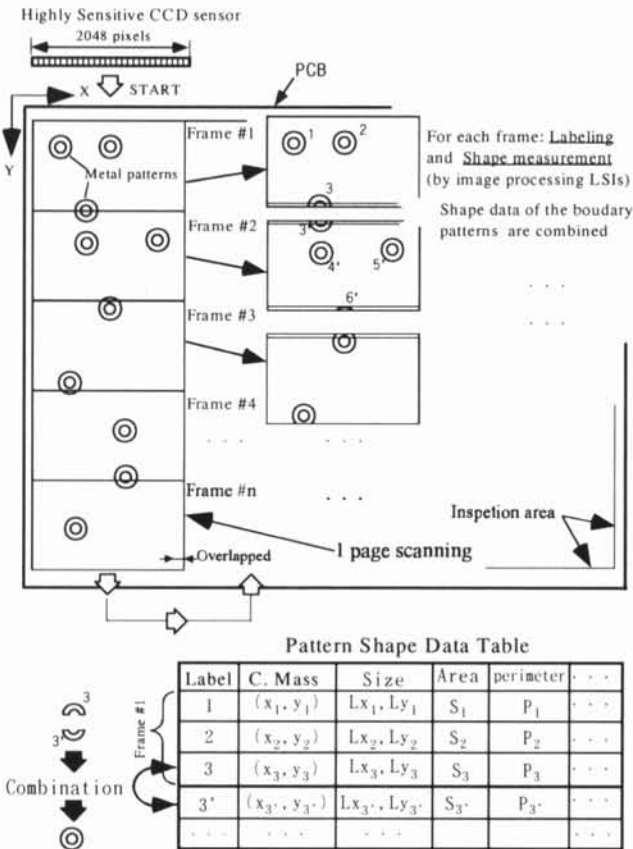


Fig. 7. Combination of the inter-frames pattern data

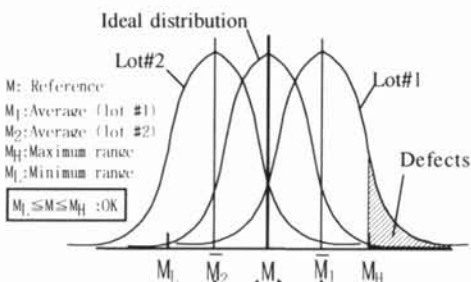


Fig. 8. Reference data compensation

patterns. These data are utilized to attribute appropriate criteria of inspection according to pattern types.

- (3) To assure the robustness concerning manufacturing process deviations, reference tables are designed with statistical considerations. Under normal conditions, patterns detected images are influenced by factors such as solder resist etching process and oxidation of pads, which cause shape data variation as shown in Figure 8. Before the inspection, the detected shape data average is calculated for each pattern type based on pattern classification codes. If the outer size average of the pattern satisfies the reference, compensation is made in the reference table, and inspection procedures are taken.

The shape measurement method described above is sufficient for detecting defects with sizes larger than the process deviation.

Output data from shape measurement and feature extraction methods are stored on a hard disk with tags for identification codes or operator's code as well as coordinates.

4.5 Comparison method for detecting printing defects

In general, inspection criteria for silk-screen printing is rougher than those for metal and solder resist pattern.

Our system for inspecting marks silk-screen printing is based on comparison of detected patterns with the pattern image generated from the CAD data used to manufacture the silk-screen. The reference pattern, which is a bit-mapped image calculated from CAD data, is generated by a workstation. This conversion is done by software and it is executed in an off-line process and stored on magnetic optical disks.

The reference pattern is divided into pages according to table scanning specifications. For the reference pattern to match the detection pattern, the original pattern from the generator is partitioned into frames, when it is loaded on the comparison hardware.

In order to perform pixel comparison for two above-mentioned images, precise alignment is essential. The fact that PCBs are subject to distortion makes the alignment problem more difficult. To overcome this problem, an alignment per frame image was realized by defining previously a pair of alignment pattern for X and Y

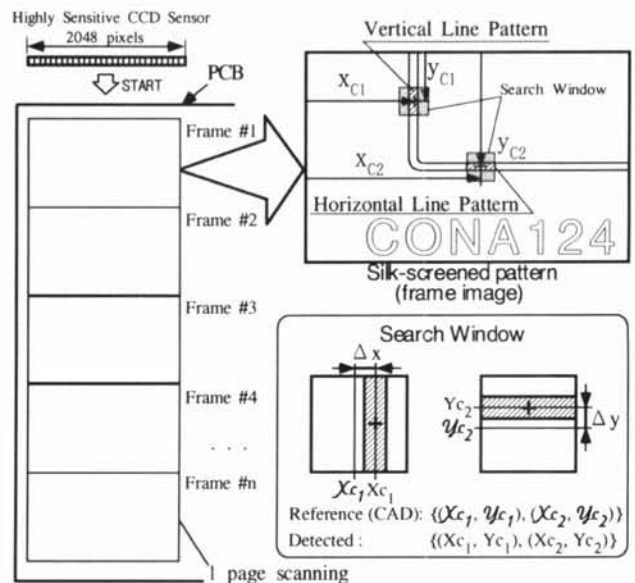


Fig. 9. Alignment of the silk-screened pattern

coordinates as shown in Figure 9. These alignment patterns and positions are determined from reference pattern of the silk-screen printing. Given that position tolerance for silk-screen printing is 0.5mm, 64x64 pixels ($\pm 0.68\text{mm}$) search windows were set. This calculation is performed in parallel and real time.

A difference image between the reference and detected image is obtained by logical EXOR operations. Small differences (noises) are wiped out from the image by a morphological contraction and expansion operation.

5. Automated inspection system

Figure 10 shows the external appearance of the developed automated inspection system. The system uses three PCs. One for general system control such as loading and unloading the inspection target board and control of the XYZ stage. Another for management of the inspection data and CAD reference data. The third one arranges the hardware for image acquirement and image processing, including the entire inspection algorithms. The PCs are networked.

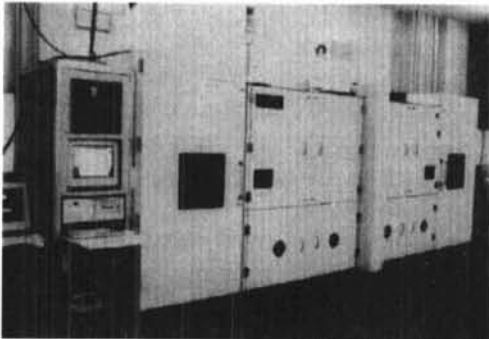


Fig. 10. External appearance of the developed system

6. Evaluation of the inspection system

According to evaluations of the developed system, gross inspection time was about 25 seconds/200x300 mm² inspection area, including board loading and unloading, position alignment, reference data loading, etc. Net inspection time for the inspection area was about 12 seconds. It was confirmed that the developed system achieves a 100% defect detection rate and has an average of 0.06% false alarms.

Figure 11 shows the results of evaluations of this system for different sized defects. The shape measurement method works well for defects greater than 70x70 μm and the feature extraction method cover defects in the range of 40x40 to 100x100 μm. Stable detection for defects greater than 50x50 μm was confirmed.

Figure 12 shows example of the detected defects. Figure 12(a) shows corner shape defect of the SMTs pad and Figure 12(b) shows a solder resist defect.

These results prove that this system can be used in actual production lines.

7. Conclusion

We developed an automated visual inspection system capable of accurately inspecting PCBs. The performance of the inspection system was evaluated and it achieved a 100% defect detection rate with a very low false alarm rate. The newly developed system increases efficiency by

making use of both shape measurement and feature extraction, thereby exploiting the strengths and overcoming weaknesses of each method. This system also provides advantages by covering a large variety of defects compared to the number of defects covered by each method alone.

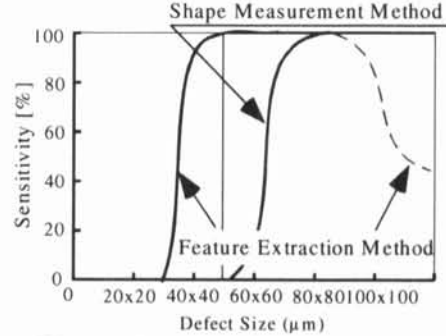


Fig. 11. Results of defect detection

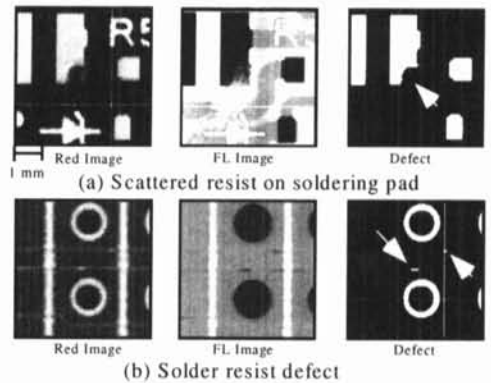


Fig. 12. Examples of detected defect

References

- [1] J. L. C. Sanz and A. K. Jain: "Machine-vision techniques for inspection of printed wiring boards and thick-film circuits," *J. Opt. Soc. Am.*, 3, 9, (1986) pp. 1465-1482
- [2] O. Mohtadi and J. L. C. Sanz : "Recent Progress in Industrial Machine Vision," *Int. J. of Robotics and Automation*, Vol. 8, No. 2, pp. 44-66
- [3] M. Moganti, F. Erkal, C. Dagli, and S. Tsunekawa : "Automatic PCB Inspection Algorithms: A Survey," *Computer Vision and Image Understanding*, Vol. 63, No. 2, (1996) pp. 287-313
- [4] T. Suzuki: "Automatic Visual Inspection Machine for Printed Circuit Boards based on Gray-scale Image Processing," *Electronic Packaging Technology*, Vol. 9, No. 12 (1993-12) pp. 40-43 (in Japanese)
- [5] N. Kaneda: "Automated Visual Inspection for Printed Circuit Boards," *The 9th Symp. of Jap. Inst. for Interconnecting and Packaging Electronics Circuits*, (1995) pp. 237-238 (in Japanese)
- [6] K. Tanimizu, S. Meguro, and A. Ishii : "High-speed Defect Detection Method for Color Printed Matter," *IECON'90 Proc.* 1, (1990-11) pp. 653-658
- [7] Y. Hara, H. Doi, K. Karasaki, and T. Iida : "A system for PCB Automated Inspection Using Fluorescent Light," *PAMI-10*, 1, (1988) pp. 69-78
- [8] Y. Hara and H. Doi : "A Method for Making the Shape of Reference Patterns Resemble the Shape of Detected Circuit Patterns," *Int. J. Japan Soc. Prec. Eng.*, Vol. 31, No. 2 (1997-6) pp. 125-129